Theory and Modeling of Edge Plasma Transport, Plasma-Wall Interactions, and Dust Dynamics

S.I. Krasheninnikov 1), A.Yu. Pigarov 1), R.D. Smirnov 1), K. Bodi 1), A.I. Smolyakov 2), D.J. Benson 1), M. Rosenberg 1), D.A. Mendis 1), T.D. Rognlien 3), T.K. Soboleva 4), W.P. West 5), B.D. Bray 5), D.L. Rudakov 1), A.L. Roquemore 6), and Y. Tanaka 7)

1) University of California at San Diego, La Jolla, California, USA
2) University of Saskatchewan, Saskatoon, Saskatchewan, Canada
3) Lawrence Livermore National Laboratory, Livermore, California, USA
4) ICN, Universidad Nacional Autónoma de México, México D. F., México
5) General Atomics, San Diego, California, USA
6) Princeton Plasma Physics Laboratory, Princeton, New Jersey, USA
7) Kanazawa University, Kakuma, Kanazawa, Japan

e-mail contact of main author: skrash@mae.ucsd.edu

Abstract. Anomalous plasma transport and plasma flows at tokamak edge, plasma-wall interactions, as well as dust dynamics and transport in fusion plasmas are among the most important processes for reactor design and performance. Recent results of theoretical studies and simulations on some aspects of these processes (including formation of meso-scale convective structures, effects of blobby transport on plasma flow in scrape-off layer, impact of wall processes and plasma-wall interactions on plasma performance, and dust dynamics and dust diagnostics) are presented and discussed in this paper.

1. Introduction

The physics of edge and Scrape-off Layer (SOL) plasmas are very complex and multifaceted. Its understanding requires physics models of anomalous plasma transport and plasma flows, plasma-wall interactions, including dust production and transport. Here, we present our recent results of theoretical studies and simulations on some important edge and SOL plasma issues.

2. Generation and dynamics of meso-scale convective structures in edge plasma

In recent years, it became clear that intermittent convective-like transport associated with meso-scale coherent structures (e.g. ELMs and blobs) are often dominant in the cross-field transport at the edge of tokamaks and stellarators [1]. The generation of ELMs is typically attributed to the peeling-ballooning instabilities, whereas the mechanism of blob formation is not clear yet. We note that in L-mode regime the edge plasma is considered to be stable with respect to the interchange drive due to stabilization by good curvature region and the magnetic field line bending (Alfven waves) as well as ion finite Larmor radius effects. Therefore, the interchange drive is not readily available as a mechanism of blob generation (contrary to what is considered in some 2D simulation models, which neglect stabilization effects). Nevertheless, in Ref. 2, 3 it was shown that the interplay of the interchange drive and nonlinear effects associated with drift wave turbulence (which is rather strong at the edge in L-mode) can lead to the blob formation. Generically, the process of formation of meso-scale structures as a result of modulational instability of drift waves has been a

subject of intensive studies for a long time (e.g. see Ref. 4 and the references therein). Our analysis of turbulent blob generation in Ref. 2, 3 is based on the application of the wave kinetic equation and the four-wave interaction approaches. Both approaches give the same result showing that the Reynolds stress, caused by small-scale drift waves, can drive large-scale ballooning mode in under-critical conditions. As an example one can see dispersion equation, Eq. (1), for ballooning mode derived with four-wave interaction approach [3].

$$\Omega^2 + \Omega\Omega_* \tau(1+\eta_i) - \Omega_{Di}\Omega_* q_\perp^{-2}\rho_s^{-2}\left(1+\eta_i+\tau^{-1}(1+\eta_e)\right) - q_z^2 v_A^2 = \\ = -2\left|\vec{e}_z\cdot(\vec{k}\times\vec{q})\right|^2\left|\phi_{\vec{k}}\right|^2\left(1+\tau^{-1}+\eta_i\right)/B_0^2 \qquad (1)$$

where Ω and $\vec{q}$ are the frequency and the wave number of ballooning mode, $\Omega_{Di,e} = q_y V_{Di,e}$, $V_{Di,e} = \pm 2\left(T_{i,e}/eB_0\right)\partial \ln B/\partial x$, $\eta_i = \partial \ln T_{0i}/\partial \ln n_0$, $\rho_s^2 = T_e/m_i\omega_{ci}^2$, $\tau = T_{0i}/T_{0e}$. In Eq. (1) the second term on the left hand side describes the drift stabilization due to finite ion temperature, the third term is the interchange drive, and the fourth term describes the Alfven stabilization. The term on the right-hand side is the Reynolds stress drive due to drift wave with the wave number $\vec{k}$ and the amplitude $\phi_{\vec{k}}$ that takes into account the diamagnetic contributions due to finite ion temperature. From Eq. (1) a simple, order of magnitude estimate was obtained for the destabilization of large amplitude, $\delta n/n_0 \sim 1$, large scale, $\Delta \sim 1/q_y$, fluctuations induced by drift waves [2]:

$$c_s^2/R\Delta - c_s^2\rho_s^2/\Delta^4 > V_A^2/q_s^2R^2, \qquad (2)$$

where we assumed $q_z \sim 1/(q_s R)$ (q_s is the safety factor and R is the tokamak major radius). The competition of the first and second terms defines the characteristic size of meso-scale structure for which the left hand side is maximal: $\Delta_m \approx (\rho_s^2 R)^{1/3}$ (we assume that $\Delta_m < L_n$, where L_n is the density scale length). Then the instability within this flux tube occurs for relatively high beta at the edge of plasma $\beta > q_s^{-2}\left(\rho_s/R\right)^{2/3}$. Recent experiments [5] qualitatively agree with such physical picture of blob generation.

It is widely accepted that an effective gravity, caused by inhomogeneous magnetic field or "neutral wind" effects, is the reason for the convective motion of meso-scale structures (e.g. see Ref. 1 and the references therein). However, it is plausible that cross-field advection of plasma structures can be associated with "spilling" of blobs into SOL/"shadow" regions due to strong turbulence and blobs can propagate further by inertia even in the absence of effective gravity. Such inertial motion of a blob in homogenous magnetic field can be described by the following 2D vorticity equation

$$\nabla\times\left(\rho(d\vec{V}/dt)\right) = \mu\nabla^2\left(\nabla\times\vec{V}\right) + \int\left(\vec{B}\cdot\nabla\right)\vec{j}\,dz/cL_b, \qquad (3)$$

where: ρ, and μ are the mass density and viscosity respectively and L_b is the blob length. The terms on the right side of Eq. (3) cause the dissipation of plasma vorticity and slow down the blob motion. As a result, blob can penetrate into SOL/"shadow" region only on some distance L_{pen}, which is determined by the initial blob speed and viscosity dissipation rate. For example, for the case where dissipation is caused by parallel current flowing through the sheath, the distance L_{pen} can be estimated as follows [1]:

$$L_{pen} \sim L_b(e\varphi_0/T)(n_b/n_{sh})(\rho_s/a_b)^3, \qquad (4)$$

where φ_0 is the initial magnitude of electrostatic potential variation in the blob, T is the plasma temperature, n_b and n_{sh} are the plasma density in the blob and in the sheath, ρ_s is the effective ion Larmor radius, and a_b is the cross-field size of the blob. For typical

conditions of the LAPD linear device: $L_b \sim 500$ cm, $\rho_s / a_b \sim 0.2$, assuming that $\varphi_0 / T \sim 1$ and $n_b / n_{sh} \sim 3$, from Eq. (4) we find $L_{pen} \sim 10$ cm.

As we see, just by inertia blob can penetrate into SOL/"shadow" region on a distance, which can significantly exceed the characteristic scale length of background plasma mass density decay $L_\rho = |\nabla \ln(\rho_{bg})|^{-1}$. However, motion of the blob involves the motion of surrounding plasma as well. If we ignore dissipative effects, total energy of plasma flow including inside and outside blob should be conserved. Then, the variation of the background plasma density in the vicinity of the blob will alter the energy of the outside flow and, therefore, should affect blob dynamics. Such effect was largely ignored in previous studies of blob physics, in particular, for the reason of the usage of the Boussinesque approximation in vorticity equation (3). Note that the total energy conservation includes the energy of the plasma motion outside the blob. This "wake" region (the size of this region is of the order of the blob radius) is imposing the force on the blob, which is causing the blob acceleration/de-acceleration in inhomogeneous plasma and is preserving the energy conservation [6]. Similar effects are observed with dipolar vortecies in 2D incompressible inhomogeneous fluid [7].

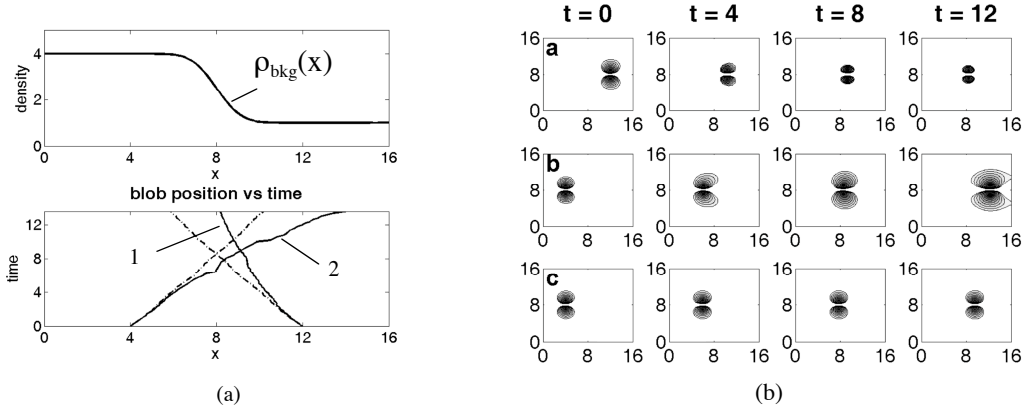

Fig. 1. (a) Top: the background plasma density profile. Bottom: dynamics of blobs initially moving towards increasing/decreasing density (curves 1/2); dotted lines correspond to blobs motion in unifrom density plasma; (b) The contours of electrostatic potential plots of a blob moving along increasing density (top), a blob moving through decreasing density (middle), and a blob moving along uniform density (bottom).

To verify analytic results the evolution of dipolar vortex of electrostatic potential seeded in incompressible inhomogeneous plasma was studied numerically by solving 2D vorticity and continuity equations. Simulations (see Fig. 1) shows blob acceleration/de-acceleration in inhomogeneous plasma, which perfectly agrees with analytic findings from Ref. 6, 7.

3. Anomalous transport and the SOL plasma flows

Near-sonic parallel plasma flows has been measured in the SOL of several tokamaks (e.g. see Ref. 8) and were modeled numerically by many authors. Study of these flows is increasingly important since they control the divertor plasma state and cause substantial impurity migration and, in the next-step fusion devices, they can enhance tritium retention and dust spreading over. Moreover, such flows determine the boundary conditions on confined plasma, have connection to X-point dependent toroidal rotation of core plasma, and can affect the L-H threshold. We used the edge plasma transport code UEDGE to study large plasma flows and different mechanisms, which can drive such flows, by

simulating experimental data from several tokamaks [9, 10]. In modeling, we include both plasma drifts and the intermittent blobby non-diffusive cross-field transport of ion species (as convection with adjustable velocity profile). We have demonstrated the dominant that the ballooning-like asymmetry of cross-field transport plays crucial role in the large (Mach~1) plasma flow formation (see C-Mod modeling results in Fig. 2 taken from [9]).

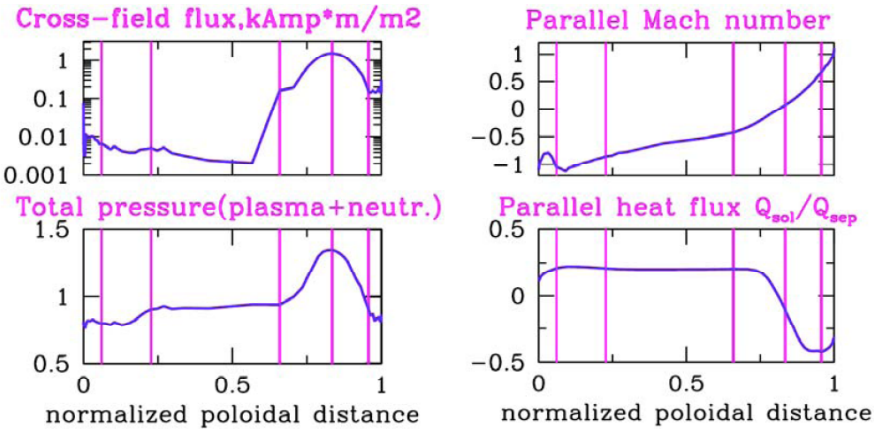

Fig. 2. Poloidal profiles of cross-field plasma flux, Mach number, total pressure, and plasma energy flux. Profiles are shown along magnetic flux surface in the far SOL. Vertical lines correspond to locations of (from left to right) entrance to inner divertor, inboard midplane, plasma top, outboard midplane, and entrance to outer divertor [9].

By fitting the data measured in both single-null and double-null magnetic configurations on C-Mod, we deduced strong asymmetry (about the factor of 10) in the plasma cross-field transport coefficients and convective velocities in the outer versus the inner SOL regions [10]. This finding is consistent with the concept of blobby SOL transport driven by bad magnetic curvature on the outer side of the torus. We also found a strong impact of large plasma flows on both impurity transport and inner leg detachment. Synergistic effect of transport asymmetries and drifts on large plasma flows in the divertor, SOL, and core plasma regions was also studied. It was found that in order to fit experimental data the amplitude of the ExB drift velocity should be reduced by the factor of 3 [10]. It is plausible that this may be related to the strong intermittency of the SOL plasma transport and corresponding inconsistency of measured and modeled averaged plasma parameters (e.g. plasma pressure, electrostatic potential, atomic rates, etc.). For example, the averaged SOL plasma pressure, which supposed to be matched by the modeling, $\langle P \rangle_m$, is the product of averaged plasma density, $\langle n \rangle$, and temperature, $\langle T \rangle$, found by the probe measurements (i.e. $\langle P \rangle_m = \langle n \rangle \langle T \rangle$). Meanwhile, due to strong intermittent character of SOL plasma transport, the actual averaged plasma pressure, $\langle P \rangle = \langle nT \rangle$, may significantly depart from $\langle P \rangle_m$.

4. Coupled plasma-wall modeling

Sophisticated integrated modeling tools are needed to describe wall erosion and re-deposition processes, and tritium retention and transport in wall materials in ITER and future magnetic fusion reactors. However, so far, there is very limited experience in the coupled plasma-wall modeling (e.g. see Ref. 11 and the references therein). Here we present newly developed transport code - the Wall and Plasma-Surface Interaction

(WALLPSI) – capable of modeling the wall temperature, erosion rates, and concentration of absorbed, mobile and trapped particle species in the wall material [12]. The code incorporates new approaches in continuum modeling of hydrogen species in wall materials, e.g. (i) modeling of dynamics and transport of specific traps produced due to chemical bond breaking and of hydrogen inventory in-there, (ii) non-diffusive transport of hydrogen species via convection directed toward the plasma facing surface in the implantation region due to nano-voids created by incident particles for a ns or longer timescales, (iii) moving plasma-facing surface interface due to erosion or deposition, and (iv) dependence of diffusion coefficient on hydrogen concentrations and on degree of material amorphization. They allow WALLPSI to properly simulate: highly non-equilibrium kinetics of hydrogen in the implantation region, retention and release of hydrogen from room up to sublimation temperatures, co-deposition, rates for chemical erosion and RES processes, and hydrogen-saturated wall conditions. The code is in the process of benchmarking against vast experimental data on hydrogen retention, permeation, and erosion rates for major fusion related materials. To study basic physics processes, WALLPSI was coupled first to our newly developed 1-D edge plasma transport code EDGE1D that mimics cross-field transport of plasma and neutrals in tokamaks with SOL by solving 5 equations (for ion and neutral atom densities and for electron, ion and neutral temperatures). The results of self-consistent plasma-neutrals-wall modeling were reported for the first time in [12] using WALLPSI/EDGE1D and showing: (i) examples of strong plasma-wall coupling, (ii) nonlinear variation of wall hydrogen inventory and recycling coefficient with respect to incident plasma flux, and (iii) the featured plasma instabilities. The details of these studies can be found in Ref. 13. Here we just highlight some findings. The build-up of trapped hydrogen inventory starting from the virgin wall material (C and Be) agrees well with experimental data from Ref. [14] (see Fig. 3 (a)). At low wall temperature even mobile hydrogen diffuses relatively slow. Moreover, accumulation of all hydrogen species in implantation region to [H]/[C]>0.4 may result in further decrease in diffusion coefficient due to H-H interactions. For consistency with experimental observations we introduce the induced convection of mobile hydrogen in the wall as $V(z) = (\Phi/N_0)\left(1 - \mathrm{erf}(z/\ell_{imp})\right)$, where z is the local depth, Φ and ℓ_{imp} are the incident flux and implantation depth, N_0 is the fitting parameter. This non-diffusive transport limits the concentrations of hydrogen at reasonable levels for $N_0 \approx 10^{29} m^{-3}$. The evolution of the profile of mobile hydrogen for graphite irradiation by 100 eV D+ is shown on Fig. 3 (b). As seen, in about a second, the concentration of mobile particles tends to become flat over implantation region and determines the saturation level. Modeling of coupled plasma-wall interactions with WALLPSI/EDGE1D shows that when the wall (C) becomes saturated with hydrogen and can switch from hydrogen wall pumping to out-gassing, the self-sustained oscillatory solutions are observed, Fig. 4 (a). Here 10-20% variation in recycling coefficient corresponds to transition between detached and hot sheath limited edge plasmas. In the case when external pumping is small, plasma evolution may end up in “thermal disruption”-like edge plasma collapse Fig. 4 (b). These oscillatory and collapse-like solutions can be triggered by thermal instability of plasma-wall interactions discussed in Ref. 15.

4. Dust in fusion plasmas

Dust is commonly found in current magnetic fusion devices. In reactors like ITER dust can pose safety hazards and impact plasma performance. However, not much is known

about the properties, generation rate, dynamics, and role of dust in fusion plasmas. In this work we analyze dynamics and statistics of dust particles as well as impact of dust-wall collisions in current tokamaks and ITER with the Dust Transport (DUSTT) code [16, 17] and compare our results with available experimental data. Here we highlight our main findings.

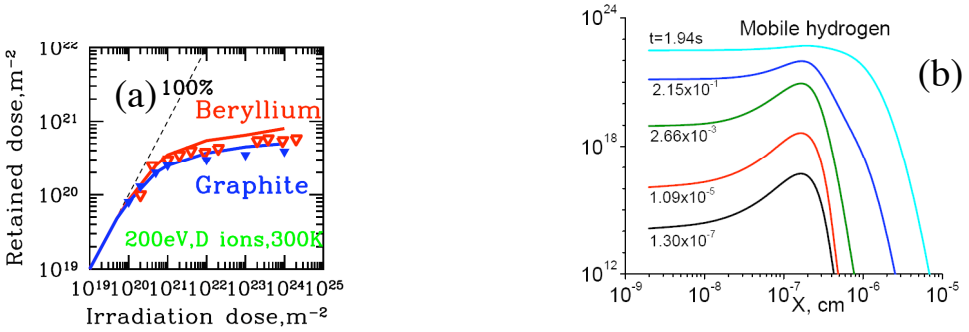

Fig. 3. (a) Comparison of WallPSI results (solid) with experimental data (triangles) for trapped D retention in C and Be. (b) Temporal evolution of the profile of mobile D in C.

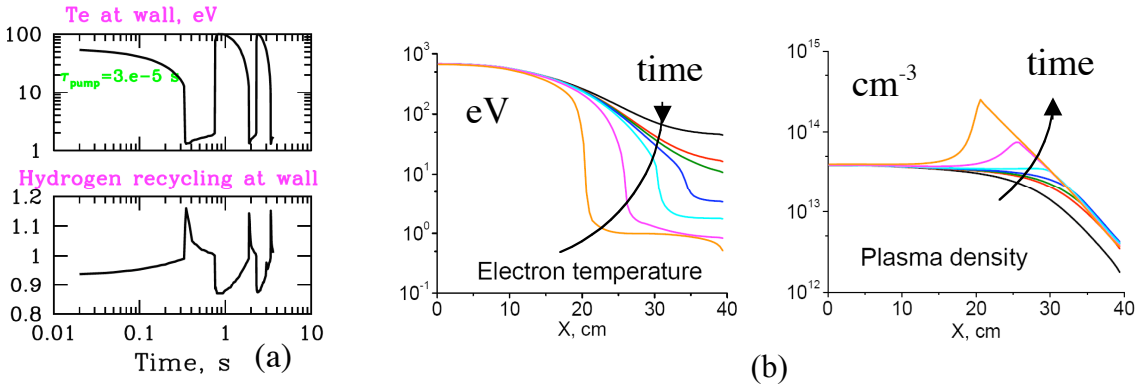

Fig. 4. (a) Self-sustained oscillations of electron plasma temperature and deuterium recycling coefficient. (b) Evolution of plasma temperature and density profiles corresponding to thermal collapse of edge plasma.

The dynamics of dust particles in tokamaks was simulated with the DUSTT code for various dust parameters and injection scenarios. A number of sample dust trajectories (initial radius 1 μm) in the DIII-D tokamak are shown in Fig. 5 (from Ref. 17). It was demonstrated that particles can be highly accelerated in the toroidal direction up to several 100m/s by dense plasma flows (see also Ref. 18) in SOL plasmas and are able to penetrate into the plasma core for several centimeters. It was shown that dynamics of dust particles in a typical SOL is governed both by the ion drag and the particle's inertia, where dust inertia prevails in the low density plasma of the far SOL and the private flux region, while the ion drag is dominant in the dense plasma regions near the separatrix. An important role of dust-wall collisions, causing the scattering of the grain and its mass and kinetic energy loss, was demonstrated.

Besides the importance of the dust-wall collisions for dust dynamics, the collisions can play a significant role in damaging of the wall surface and secondary dust production. We use the LS-DYNA, the commercial finite element program for structural analysis, and consider the collisions of beryllium and tungsten spherical dust particles with a beryllium flat surface [19]. We found that at low speeds ~100m/s no significant damage to the wall occurs. Dust grains reflect from the wall with the restitution coefficient ~0.2 and can be

partially destroyed on the collision. At high impact speed ~1km/s beryllium dust is completely destroyed upon colliding, forming a cone of debris material injected into the plasma, Fig. 6 (a). At the same speed the tungsten dust causes significant damage to the wall forming large crater at the wall, Fig. 6 (b) [19].

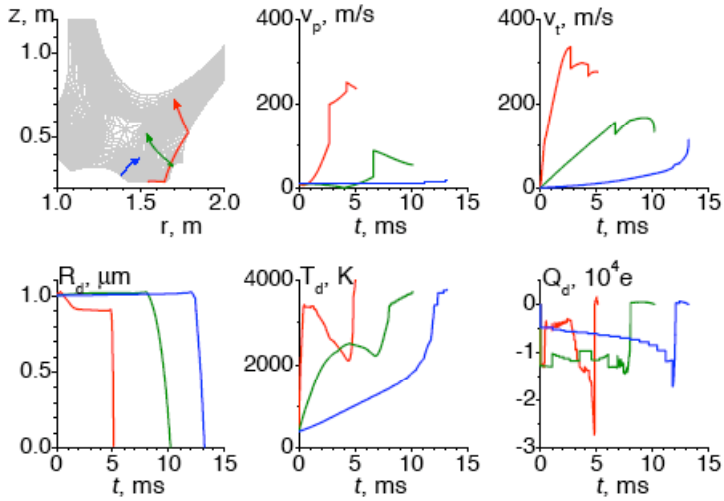

Fig. 5 .The simulated sample trajectories and time variations of dust radius, R_d*; poloidal,* V_p*, and toroidal,* V_t*, velocities; temperature,* T_d*, and charge,* Q_d*, in DIII-D tokamak.*

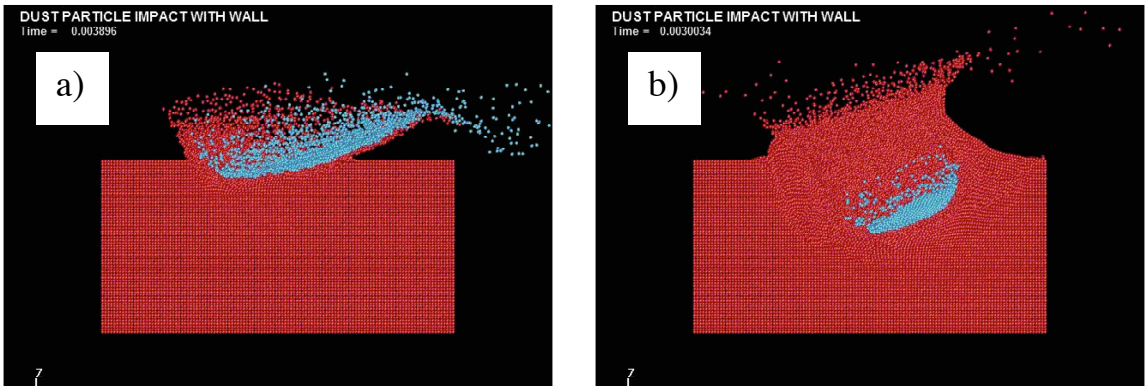

Fig. 6. Simulated impact of beryllium (a) and tungsten (b) dust particle of radius 0.5 mm on beryllium wall at speed 1 km/s and angle 45° to the wall normal.

We have also performed refined analysis of dust radius distribution resulting from laser scattering measurements on DIII-D taking into account non-Rayleigh regimes of light scattering as well as dust evaporation due to heating by laser radiation [20]. As a result, we found that the re-evaluated dust radii are in the range 50-800 nm with the mean dust radius ~170 nm (an increase by about a factor of 2 as compared to the previous evaluations based on Rayleigh approximation [21]), while the re-evaluated radius of the mean dust volume increased to ~250 nm. It was also shown that the obtained dust radius distribution decreases more slowly than R_d^{-3} in the range of measured radii, therefore much of the total dust mass is carried by big particles. This brings us to the following issues. Our current estimates of dust-plasma interactions including charging, heat fluxes to the grain, etc. are based on the Orbit Motion Limited theory. However, high dust temperature causes intense ablation of the grain material and the presence of the vapor can significantly alter the interactions of plasma with the dust grain because the vapor can shield the grain from the plasma in a manner somewhat similar to that in pellet-plasma

interactions. As a crude estimate of the parameter range where one can expect significant impact of the vapor we can consider the effects of both ion-vapor collisions and electron impact ionization of the vapor. Vapor density can be found from the grain energy balance equation taking into account grain heating by the plasma and cooling by radiation loss and evaporation. Then we find that for rather "large" dust grains, $R_d \gtrsim 30-100\,\mu m$, plasma-vapor interactions become important and standard OML theory and corresponding numerical modeling cannot be used [22].

The vapor issue is also important for the interpretation of the fast camera images of dust: what do we actually see on the camera? Is it the image of the grain due to the grain's thermal radiation or it is the image of the plume formed by grain's ablation and emitting light due to the electron impact excitation of plume neutrals and ions? And, finally, what minimal grain size is visible? The analysis of radiation and ablation processes shows that in most current experimental cases minimal visible grain size is about a few μm; in the SOL and divertor regions the main radiation is due to thermal radiation of the grain, while in the regions close to and inside the separatrix plume radiation prevails [23].

Acknowledgement. This work was supported in part by U.S. Department of Energy under grants DE-FG02-04ER54739, DE-FG02-06ER54852, and DE-FC02-07ER54908 at University of California, San Diego.

References

[1] KRASHENINNIKOV, S. I., et al., J. Plasma Phys. published online Jan 2, 2008 (2008)
[2] KRASHENINNIKOV, S. I., SMOLYAKOV, A. I., Phys. Plasmas **14**, 102503 (2007)
[3] SMOLYAKOV, A. I., KRASHENINNIKOV, S. I., Phys. Plasmas **15**, 072302 (2008)
[4] DIAMOND, P. H., et al., Plasma Phys. Control. Fusion **47**, R35 (2005)
[5] LABOMBARD, B., et al., Nucl. Fusion **45**, 1658 (2005)
[6] BODI, K., et al., submitted to Phys. Plasmas (2008)
[7] EAMES, I., HUNT, J.C., J. Fluid Mech. **353**, 331 (1997)
[8] LABOMBARD , B., et al., Nucl. Fusion 44, 1047 (2004)
[9] PIGAROV, A.Yu., et al., Contrib. Plasma Phys. **46**, 229 (2006)
[10] PIGAROV, A.Yu., et al., J. Nucl. Materials **363**, 643 (2007)
[11] FEDERICI, G., et al., Nucl. Fusion **41**, 1967 (2001)
[12] PIGAROV, A.Yu., et al., "Coupled plasma-wall modelling", Proceedings of 18th Int. Conf. on Plasma-Surface Interactions (Spain, May 2008), submitted to J. Nucl. Mater.
[13] PIGAROV, A.Yu., KRASHENINNIKOV, S. I., submitted to Phys. Plasmas (2008)
[14] ROTH, J., J. of Physics: Conference Series **100**, 062003 (2008)
[15] KRASHENINNIKOV, S. I., SOBOLEVA, T.K., Phys. Plasmas **13**, 094502 (2006)
[16] PIGAROV, A.Yu., et al., Phys. Plasmas 1**2**, 122508 (2005)
[17] SMIRNOV, R.D., et al., Plasma Phys. Control. Fusion **49**, 347 (2007)
[18] KRASHENINNIKOV, S. I., et al., Phys. Plasmas **11**, 3141 (2004)
[19] SMIRNOV, R.D., et al., "Modeling of velocity distributions of dust in tokamak edge plasmas and dust-wall collisions", Proceedings of 18th Int. Conf. on Plasma-Surface Interactions (Spain, May 2008), submitted to J. Nucl. Materials.
[20] SMIRNOV, R.D., et al., Phys. Plasmas **14**, 112507 (2007)
[21] WEST, W. P., et al., Plasma Phys. Control. Fusion **48**, 1661 (2006); WEST, W. P., BRAY, B. D., J. Nucl. Materials **363-365**, 107 (2007)
[22] KRASHENINNIKOV, S. I., et al., submitted to Plasma Phys. Control. Fusion (2008)
[23] SMIRNOV, R.D., et al., submitted to Phys. Plasmas (2008)